engineering proceedings

MDPI

Proceedings Paper

Development of a Novel MEMS Gas Flowmeter with a Temperature Difference Suspension Structure †

Basit Abdul [1,*], Abdul Qadeer [2] and Abdul Rab Asary [3]

[1] Institut Interdisciplinaire d'Innovation Technologique (3IT), 3000, Boul, Université, Sherbrooke, QC J1K 0A5, Canada

[2] The University of Lahore, Pakistan; qadeer.abdul54321@gmail.com

[3] Laboratoire d'Ingénierie des Fluides et des Systèmes Énergétiques—LIFSE, Arts et Métiers Institute of Technology Paris, 151 Boulevard de l'Hôpital, 75013 Paris, France; abdulrabasary@hotmail.com

* Correspondence: basit.abdul@usherbrooke.ca

† Presented at The 11th International Electronic Conference on Sensors and Applications (ECSA-11), 26–28 November 2024; Available online: https://sciforum.net/event/ecsa-11.

Abstract: Micro-electro-mechanical systems (MEMS) gas flowmeters are innovative devices that use microfabrication technology to measure gas flow with high precision and sensitivity. With MEMS technology, flow measurement can now be performed more accurately and compactly than ever, using low-power, compact, and highly accurate sensors. MEMS gas flowmeters utilize various principles to measure gas flow, including thermal, Coriolis, and pressure differential methods. A micro flowmeter was developed by combining a MEMS sensor with a weak signal acquisition technique. High heat isolation and sensitivity can be achieved using a MEMS sensor with a thermal resistor-suspended VO_2 structure. Since SU-8 gum was used for the flow channel, the technology was simple and affordable, making it suitable for batch production. To acquire high-resolution, low-noise data, the following device used a super low bias current operational amplifier, aided by Guard ring protection, and a 24-bit high-resolution ADC. The sensor and data acquisition combination shows the flow meter has favorable linearity and sensitivity between 0 and 50 mL/min at a specific offset voltage. Biochemical detection and medicine require a high sensitivity, stability, and low-cost flow meter.

Keywords: micro flowmeter; MEMS; thermal resistor suspended structure; weak signal acquisition; high-resolution ADC

Citation: Abdul, B.; Qadeer, A.; Asary, A.R. Development of a Novel MEMS Gas Flowmeter with a Temperature Difference Suspension Structure. *Eng. Proc.* **2024**, *6*, x. https://doi.org/10.3390/xxxxx

Academic Editor(s):

Published: 26 November 2024

Copyright: © 2024 by the authors. Submitted for possible open access publication under the terms and conditions of the Creative Commons Attribution (CC BY) license (https://creativecommons.org/licenses/by/4.0/).

1. Introduction

The MEMS system comprises a micro sensor, DSP, power, and specific function. Due to its small volume, low power consumption, and delicate operation, nanoscience is becoming increasingly dependent on this technology [1]. In fields like biochemistry and medicine, flow sensors must be able to operate at high precision, at a minimal volume, and with a very short response time since flow rates generally range from L/min to mL/min. During the past few years, there has been an increasing interest in flow sensors based on MEMS technology because of their inherent characteristics [2]. Innovative MEMS sensors for underwater applications and communications systems have been reported [3–12].

To detect tiny flows, signal acquisition systems in this type of flowmeter should have high resolution, for example, 0.01 mL/min. Thus, designing a signal acquisition system that is low noise and high-resolution is essential. This paper proposes designing and fabricating a micro gas flow sensor using the MEMS technique and designing and fabricating a low-noise, high-resolution signal acquisition system, which directly correlates with the sensor's output. The flow meter must possess some specific advantages, such as high

sensitivity and stability, to satisfy the needs of the applications in biochemical detection and medicine. Furthermore, it should also be cost-effective.

2. Overall Design

Figure 1 illustrates the overall structure of the microflowmeter system. The MEMS sensor produces a weak voltage signal depending on the gas flow. A high-resolution ADC is used to sample a weak voltage signal, after which a low-noise operational amplifier amplifies it, and the amplitude of the signal is then acquired by the MCU, which in turn is used to calculate the corresponding flow velocity based on the sampled signal. Using a serial port or an LCD display, the measurement results can be displayed and transferred to the underlying computer to simultaneously display the curves for the measurements.

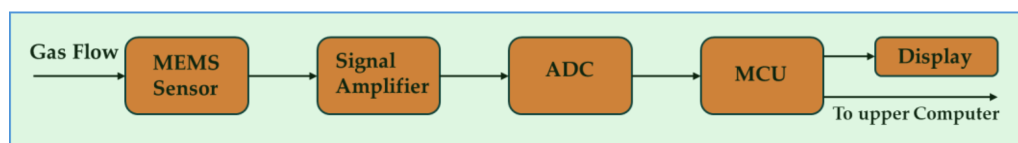

Figure 1. Micro Flowmeter System Structure.

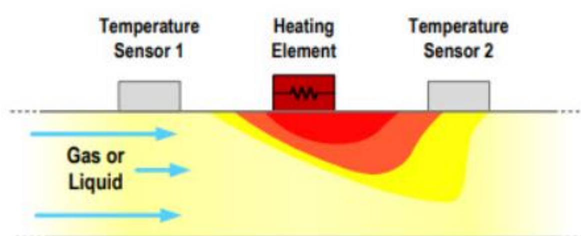

Figure 2. Micro Flowmeter System Structure.

Flow meters represent the instrumentation of flow sensors and are used to measure the amount of flow that passes through them. There are in principle five different flow meter types: velocity flow, positive displacement flow, differential pressure flow, open channel flow, and mass flow. Gas flow meters are one of the dominant types due to their faster response and better accuracy than other flow meters. They can also be effectively miniaturized and manufactured on silicon wafers. The emergence of MEMS has already revolutionized the consumer electronics market for motion, pressure, and other sensors, and similar micro-machining processes are now being adapted to fabricate flow sensors. Flow sensing applications are typically high-mix and low-to-medium volume compared, for example, to motion sensors that have become ubiquitous in hundreds of millions of smartphones. This novel MEMS gas flowmeter with a temperature difference suspension structure is designed to achieve high sensitivity, low power consumption, and precision in measuring gas flow rates.

3. Sensor Design

3.1. Operational Principle of Sensor

In differential calorimetric flow sensors, thermal resistors are placed on both ends. During gas flow, the heat distribution map created by the heat source moves, which changes the resistance of upper and lower resistors. Based on this change, the gas flow velocity can be calculated. Usually, a Wheatstone bridge is used to perform the estimation, as shown in Figure 3 [13].

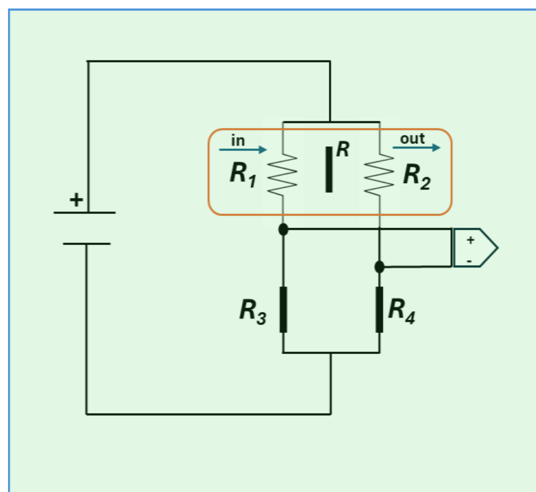

Figure 3. Schematic representation of Wheatstone bridge.

It demonstrates [14] that determining the output voltage of a bridge is a complex function that includes parameters for flow velocity, structure, and material characteristics.

3.2. Fabrication Process

Two thermal resistors are suspended in a flow channel in this flow sensor, forming a thermal resistor-suspended structure. Unlike conventional structures, this structure has no conduction from the base, which makes it highly effective at isolating heat. Consequently, it has a high degree of sensitivity and rapid response time. 3R and 4R are precision resistors that remain stable regardless of temperature. We chose VO2, which has a high resistor temperature coefficient, to prepare thermal resistors with a higher sensitivity. Due to VO2's temperature coefficient of -3.4×10^{-2} K^{-1}~4×10^{-2} K^{-1} (Pt's TCR is -3.9×10^{-3} K^{-1}), the output voltage increases, resulting in a higher sensitivity. Aside from that, VO2 is chemically inert, making it ideal for the stabilization of sensor electrodes [15]. Figure 4 shows the sensor's MEMS fabrication process.

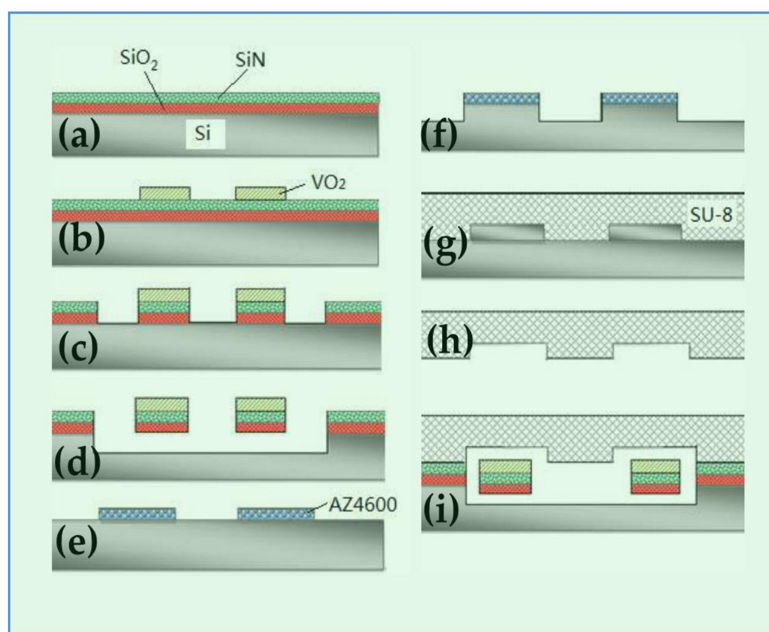

Figure 4. MEMS Fabrication Process.

The fabrication process is described below.

1. The oxide layer of SiO_2 is deposited on the silicon base. LPCVD is then used to deposit a layer of Si_3N_4 as the thermal resistor-bearing beam.
2. The thermal resistor graph will appear after exposure.
3. After lifting off, deposit VO2 and obtain thermal resistors.
4. Photolithography is used to fabricate the flow channel graphic, which is covered with positive photoresist. Release the thermal resistors by combining mechanical erosion and corrosion with KOH.
5. To get the SU-8 gum mold graph, cover AZ4600 gum on the silicon chip.
6. By mechanical deep erosion, obtain SU-8 gum mold.
7. After the SU-8 gum has solidified, generate the microchannels.
8. Microchannels in SU-8 gum should be aligned with those in silicon chips.

4. Acquisition System Design

4.1. Guarding of Amplifying Circuit

The amplifier's gain and noise performance affect measurements' precision and resolution. Here, we use a low-biased current amplifier, the LMP7721. In addition to a bias current limited to ±20fA, the amplifier also possesses an offset voltage below 26 uV [16]. As a result of pollution or humidity, PCB resistivity decreases. Thus, leakage current will occur at the input point due to potential differences between the input and other stations, which cannot be ignored when detecting weak signals. Problems like this can be solved with the Guard method. A guard is present at the sensitive node. It comprises a low-impedance conductor with a potential raised to match the node's voltage. The Guard Ring passes the leakage current to the analog ground without interfering with the input [17]. To prevent leakage currents, the LMP7721 needs to be fully guarded.

4.2. High-Resolution ADC

It is necessary to have a high-precision ADC to acquire high-precision signals. Here, we used the ADS1211, a four-channel, 24-bit high-precision ADC manufactured by B.B. Corporation. ADS1211's effective resolution is 20 bits, and a low noise programmable gain amplifier further enhances the dynamic range [18]. For 5V, the theoretical resolution would be 5000/220 = 0.005 mV.

4.3. Power and Layout

Power supplies, DC-DC ICs, and disturbances from digital to analog supplies generate considerable power noise. DC-DC ICs and batteries with low noise are recommended to attenuate this type of noise. Separate power should be provided for analog and digital components. A disturbance is isolated by putting an inductance between the AVDD and DVDD if only one power supply is used [19].

In addition to the arrangement and wiring of the PCB, these factors strongly influence the noise of the acquisition system. First, analog and digital devices should be arranged separately. Second, there should be sufficient width between power lines to prevent the spread of resistance and inductance. Lastly, the grounds for the digital and analog parts must be laid separately and then connected via magnetic beads.

5. Experiment Results and Analysis

Figure 5 shows the velocity-output curve when the offset voltage is 10 V, 12 V, and 14 V. The increased output voltage from a higher offset voltage enhances sensitivity in the 1~50 mL/min range. The linearity range, however, decreases as the offset voltage increases. If an offset voltage of 14V is applied, the linear range increases to 25 mL/min.

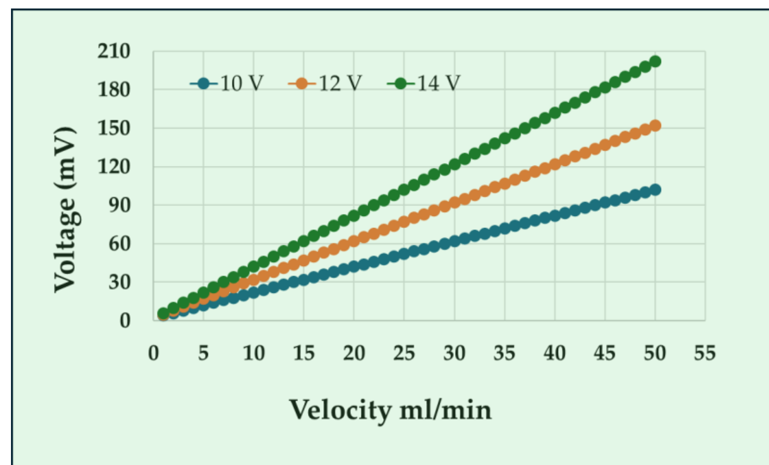

Figure 5. A comparison of response characteristics under different offsets.

6. Conclusions

This paper describes the design of a microflowmeter that includes a sensor and a data acquisition module. As a flow sensor, this device is fabricated through MEMS technology, with a thermal resistor suspended in its structure. It also has excellent temperature isolation capabilities. SU-8 gum is used in the flow. In addition to being simple, highly stable, and suitable for bulk production, this technology is also cost-effective. The weak signal is amplified by a super low bias current operational amplifier, LMP7721, combined with a Guard Ring. Data is acquired using the 24-bit ADS1211 manufactured by B.B. Company. It is necessary to separate analog from digital parts, ground them separately, and isolate disturbances from digital to analog. Data acquisition and sensor combination indicate that the flowmeter is linear and sensitivity-conforming in the range of 0-50mL/min at a suitable offset voltage. As a result, it is suitable for biochemical detection, medicine, etc., providing good prospects for promotion.

Author Contributions: Conceptualization, B.A. and A.Q.; methodology, B.A.; software, B.A., A.Q.; validation, B.A., A.Q. and A.R.S.; formal analysis, A.R.S.; investigation, B.A.; resources, B.A.; data curation, B.A. and A.R.S.; writing—original draft preparation, B.A.; writing—review and editing, B.A., A.Q. and A.R.S.; visualization, A.Q.; supervision, B.A.; project administration, B.A. All authors have read and agreed to the published version of the manuscript.

Funding: This research received no external funding.

Institutional Review Board Statement: Not applicable.

Informed Consent Statement: Not applicable.

Data Availability Statement: The data presented in this study are available within the article and there is presented in every graph. There is no more data apart from the presented.

Conflicts of Interest: The authors declare no conflict of interest.

References

1. Huang, L. Micromachined Thermal Time-of-Flight Flow Sensors and Their Applications. *Micromachines* **2022**, *13*, 1729. https://doi.org/10.3390/mi13101729.
2. Löfdahl, L.; Gad-El-Hak, M. MEMS applications in turbulence and flow control. *Prog. Aerosp. Sci.* **1999**, *35*, 101–203. https://doi.org/10.1016/s0376-0421(98)00012-8.
3. Abdul, B.; Mastronardi, V.; Qualtieri, A.; Guido, F.; Algieri, L.; Rizzi, F.; De Vittorio, M. Design, fabrication and characterization of piezoelectric cantilever MEMS for underwater application. *Micro Nano Eng.* **2020**, *7*, 100050. https://doi.org/10.1016/j.mne.2020.100050.
4. Abdul, B.; Mastronardi, V.M.; Qualtieri, A.; Algieri, L.; Guido, F.; Rizzi, F.; De Vittorio, M. Sensitivity and Directivity Analysis of Piezoelectric Ultrasonic Cantilever-Based MEMS Hydrophone for Underwater Applications. *J. Mar. Sci. Eng.* **2020**, *8*, 784. https://doi.org/10.3390/jmse8100784.

5. Abdul, B.; Abdul, S.; Asary, A.R. Biomimetic Cilia-based MEMS Sensors for Underwater Applications—A Review. *North Am. Acad. Res.* **2021**, *4*, 11–21. https://doi.org/10.5281/zenodo.5768208
6. Abdul, B.; Shibly, M.A.; Asary, A.R. Development of a Cochlear Biomodel using Micro-Electromechanical Systems (MEMS). In Proceedings of the 10th International Electronic Conference on Sensors and Applications, 15–30 November 2023, Basel, Switzerland. https://doi.org/10.3390/ecsa-10-15995.
7. Abdul, B.; Shibly, M.A.H.; Asary, A.R. Development of a Novel Design and Modeling of MEMS Piezoelectric Cantilever-Based Chemical Sensors. *Eng. Proc.* **2023**, *56*, 105. https://doi.org/10.3390/ASEC2023-15356.
8. Abdul, B. Development of a Novel Silicon Membrane MEMS Capacitive Pressure Sensor for Biological Applications. *Eng. Proc.* **2023**, *48*, 54. https://doi.org/10.3390/CSAC2023-15170.
9. Abdul, B.; Shibly, M.A.H.; Asary, A.R.; Ruma, N.J. Design and Modelling of MEMS Resonators for an Artificial Basilar Membrane. *Eng. Proc.* **2023**, *48*, 15. https://doi.org/10.3390/CSAC2023-14896.
10. Abdul, B.; Shibly, M.A.H.; Asary, A.R. Combining COMSOL Modeling with Different Piezoelectric Materials to Design MEMS Cantilevers for Marine Sensing Robotics. *Eng. Proc.* **2023**, *37*, 64. https://doi.org/10.3390/ECP2023-14641.
11. Asary, A.R.; Abdul, B.; Samad, A.; Shibly, M.A.H. Enhancing Gamma Stirling Engine Performance through Genetic Algorithm Technique. *Eng. Proc.* **2023**, *56*, 29. https://doi.org/10.3390/ASEC2023-15264.
12. Sadiq, H.; Sadiq, H.; Sohail, A.; Basit, A.; Akhtar, N.; Batool, K.; Hisaindee, S.; Asghar, L. Assessment of antioxidant activity of pure graphene oxide (GO) and composite V2O5/GO using DPPH radical and H2O2 scavenging assays. *J. Sol-Gel Sci. Technol.* **2023**, *108*, 840–849. https://doi.org/10.1007/s10971-023-06231-6.
13. Kuo, J.T.W.; Yu, L.; Meng, E. Micromachined Thermal Flow Sensors—A Review. *Micromachines* **2012**, *3*, 550–573. https://doi.org/10.3390/mi3030550.
14. Nguyen, N.; Dötzel, W. Asymmetrical locations of heaters and sensors relative to each other using heater arrays: a novel method for designing multi-range electrocaloric mass-flow sensors. *Sensors Actuators A: Phys.* **1997**, *62*, 506–512. https://doi.org/10.1016/s0924-4247(97)01529-x.
15. Wang, L.; Li, J. Fabrication of Vanadium Dioxide Films at Low Temperature and Researches on Properties of the Films. *Acta. Phys.* 2006, 55, 2846-2851. (In Chinese)
16. National Semiconductor Corporation. 3 Femtoampere Input Bias Current Precision Amplifier LMP7721. 2008. Available online: http://www.national.com (accessed on 23 July 2024).
17. Li, H. Design of a MEMS Temperature Difference Suspended Structure Gas Flowmeter. *Appl. Mech. Mater.* **2012**, *268–270*, 1548–1552. https://doi.org/10.4028/www.scientific.net/amm.268-270.1548.
18. Burr-Brown Corporation. 24-Bit ANALOG-TO-DIGITAL CONVERTER ADS1211[R]. 2007. Available online: http://www.burr-brown.com (accessed on 23 July 2024).
19. Montrose Mark, I. Printed Circuit Board Design Techniques for EMC[M]; Wiley-IEEE Press: Hoboken, NJ, USA, 2010.

Disclaimer/Publisher's Note: The statements, opinions and data contained in all publications are solely those of the individual author(s) and contributor(s) and not of MDPI and/or the editor(s). MDPI and/or the editor(s) disclaim responsibility for any injury to people or property resulting from any ideas, methods, instructions or products referred to in the content.